Journal of Newviews in Engineering and Technology (JNET)
Volume 5, Issue 4, December 2023
Available online at http://www.rsujnet.org/index.php/publications/2023-edition
e- ISSN: 2795-2215

Exergy and Non-linear Gas Path Analysis of a Gas Turbine Power Plant

Nkoi, B., Adike, J. A. and Lebele-Alawa, B. T.
Department of Mechanical Engineering, Rivers State University, Nkpolu-Oroworukwo, Port Harcourt, Nigeria
joseph.adike@ust.edu.ng ; nkoi.barinyima@ust.edu.ng

ABSTRACT
An exergy and non-linear gas path analysis was carried out on a 180 MW gas turbine power plant in Afam, Rivers State, Nigeria. The plant major components were separated into control volumes of exergy inflows and outflows, then analyzing each flow using the first and second laws of thermodynamics. For non-linear gas path analysis, the thermodynamic relationship between engine gas path measurement parameters and engine component parameters was modeled at base load conditions. The power plant's overall average net efficiency was 36.997 percent, according to the findings. The turbine has the lowest exergy loss rate at 15.86 percent, while the combustion chamber has the greatest loss rate at 38.88 percent. The average actual and calculated turbine inlet temperatures were found to differ by 0.30 percent in the study. With a deviation of 9.672 percent, the average actual turbine exit temperature was higher than expected, which was attributed to non-utilization of available energy due to turbine inter-stage leakages. The machine path components' performance is limited by the deteriorated performance caused by tear and wear effects. The assessment performed revealed areas of high exergy losses and component part degradation with the intention of improving plant efficiency by implementing good maintenance practice and utilizing the heat in exhaust gases to generate steam with no supplementary fuel burning to increase electric power output.

KEYWORDS: Efficiency, Exergy analysis, Gas path analysis (GPA), energy loss rate, gas turbine.

Cite This Paper: Nkoi, B., Adike, J. A., & Lebele-Alawa, B.T. (2023) Exergy and Non-linear Gas Path Analysis of a Gas Turbine Power Plant. *Journal of Newviews in Engineering and Technology*. 5(4), 15 – 27.

1.0 INTRODUCTION

Component efficiencies and turbine working temperature have an impact on gas turbine performance. In real gas turbine processes, however, the acceleration and compression of the working fluid results in some energy loss due to friction and irreversibility (Lebele-Alawa & Asuo, 2011). Furthermore, friction causes pressure loss during the combustion of the working fluid. Finally, unlike in an ideal cycle, the actual expansion of the working fluid and the actual extraction of energy by the turbine are not isentropic. Friction, irreversibility, and inefficiencies caused by the various components result in energy loss and degradation of gas path component performance. The operating conditions of the gas turbine module are typically measured to calculate output power and efficiency (Horlock, 2003).

The combustion chamber, turbine section, and exhaust part are all components of the hot gas path (Stamatis, 2010). The parts in the hot gas path, such as combustors, blades, and vanes, must be optimized because they must withstand harsh operating conditions. During operation, gas path components are vulnerable to a variety of problems such as fouling, erosion, corrosion, increased tip clearance, and object damage, among others (Verbist, 2017). These issues also have the potential to reduce the machine's performance.

In this study, the components performance deviations of the Afam GT13E2 power plant are investigated to maximize energy efficiency and

Journal of Newviews in Engineering and Technology (JNET)
Volume 5, Issue 4, December 2023
Available online at http://www.rsujnet.org/index.php/publications/2023-edition
e- ISSN: 2795-2215

minimize losses, using exergy and non-linear gas path analysis models to reveal areas of high energy losses and component part degradation with the prior intention of improving plant efficiency by implementing good maintenance practices and utilizing the heat in the exhaust gases to generate steam without the use of supplementary fuel to increase power generated. According to Parapa (2021), the analysis concludes that changes in exhaust temperature parameter of 1^{0C} has an impact on decreasing the power output by 0.273% and increasing the heat rate by 0.047%. When the performance degradation is small, it is difficult to detect. According to Yulong *et al*. (2015), the model-based GPA method has been widely used to monitor gas turbine engine health status because it can easily obtain the magnitudes of detected component faults using a thermodynamic performance model that relates gas path measurable (dependent) parameters such as temperatures, pressures, and shaft rotational speeds, among others, to fundamental component performance (independent) parameters.

Energy balance is the traditional method of assessing the energy of an operation involving physical and chemical analysis, as well as mass conservation of energy. This energy balance appears to be based on the first law of thermodynamics, and as such, system information is adapted to help eliminate heat losses or improve heat recovery. However, there is insufficient data on energy system degradation from such energy balances. Although the non-linear gas path model indicates system degradation (unhealthy state), it only states the magnitude of heat lost and not the quality of heat streams lost across system component boundaries.

Baheta and Gilani (2011), investigates exergy-based performance analysis of a gas turbine at part-load conditions which results shows high exergy destruction rates in the combustion chamber and exhaust using staggering variable stator vanes. Investigation of the effects of load variation and ambient temperature from 21^{0C} to 33^{0C} reveals that the turbine has the highest exergy efficiency of the plant (Okechukwu & Imuentinyan, 2013).

The exergy method aids in overcoming the first law's limitation. The concept of exergy is founded on the first and second laws of thermodynamics. Exergy analysis identifies the locations of energy degradation, as well as the causes and magnitudes of exergy losses in the system (Oyedepo *et al*, 2015). This approach provides a common scale for comparing component performances, which may lead to improved operation and maintenance and increased unit efficiency.

2.0 MATERIALS AND METHODS

2.1 General Plant Description

Afam Power Plant is located in Oyigbo in Rivers State, Nigeria. It is a 180 MW single shaft ALSTOM GT13E2 unit gas turbine power plant that uses low heating value natural gas and operates on the Brayton cycle.

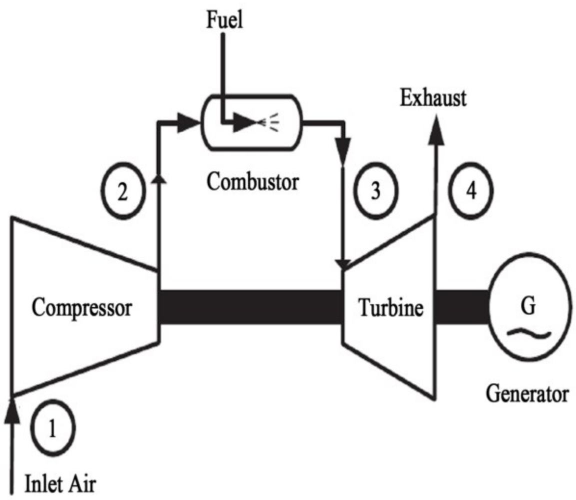

Figure 1. Schematic of a single shaft gas turbine

Journal of Newviews in Engineering and Technology (JNET)
Volume 5, Issue 4, December 2023
Available online at http://www.rsujnet.org/index.php/publications/2023-edition
e- ISSN: 2795-2215

The main mechanical parts consist of a combustion chamber between the compressor and the turbine, a 5-stage turbine, and a 21-stage axial compressor mounted on the same shaft. The exhaust flow is 528 kg/s at 3000 rpm, the fuel mass flow rate is 9.1 kg/s, and maximum combustor temperature is 1368 K.

2.2 Methods

For ease of analysis and illustration, the two approaches used in this study are typical for open cycle gas turbine systems. The gas turbine power plant was divided into various control volumes, and energy and exergy balances were performed using the first and second laws of thermodynamics for each significant system component. To calculate the necessary parameters that cannot be measured directly, either locally in the field or remotely from the human-machine interface and control systems, MATLAB Ra2016 and Microsoft 365 excel software were used. The thermodynamic relationship between engine gas path measurement parameters and engine component parameters was modeled at base load conditions for non-linear gas path analysis.

2.3 Energy Model

Isentropic compression:

$$W_C = m_a C_{pa}(T_2 - T_1) \tag{1}$$

$$T_2 - T_1 = \frac{T_1\left(r_P^{\frac{\gamma-1}{\gamma}} - 1\right)}{\eta_C} \tag{2}$$

$$W_C = m_a C_{pa} T_1 \left\{ \frac{\left(r_P^{\frac{\gamma-1}{\gamma}} - 1\right)}{\eta_C} \right\} \tag{3}$$

Compressor isentropic efficiency

$$= \eta_C = \frac{T_{2s} - T_1}{T_2 - T_1} \tag{4}$$

Heat addition in combustion chamber:

$$Q_{CMB} = [m_a C_{pa} + m_a C_{pa}](T_3 - T_2) \tag{5}$$

Turbine heat supply

$$W_T = [m_a C_{pa} + m_a C_{pa}](T_3 - T_4) \tag{6}$$

Turbine isentropic efficiency

$$= \eta_T = \frac{T_3 - T_4}{T_3 - T4s} \tag{7}$$

2.4 Exergy model

Exergy analysis entails combining the first and second laws of thermodynamics. Exergy analysis uses the same set of equations for all hot gas path components, ignoring differences in the internal thermodynamic cycle of the components. This method provides a common scale for comparing the performances of thermodynamic components.

From first law of thermodynamics,

$$dQ = du + pdv \tag{8}$$

From second law of thermodynamics

$$(dQ)_{rev} = Tds$$

Also, $h = u + pv$ (9)

$$dh = du + d(pv)$$

$$dh = du + pdv + vdp \tag{10}$$

For constant volume process

$$pdv = 0$$

$$dh = du + vdp$$

$$\therefore Tds = dh - vdp \tag{11}$$

Or

$$dQ = dH - Vdp = C_p dT - \frac{RT}{p} dp \tag{12}$$

$$dH = C_p dT$$

$$dS = C_p \frac{dT}{T} - R\frac{dp}{p}$$

$$s_2 - s_1 = C_p \ln\frac{T_2}{T_1} - R\frac{p_2}{p_1} \tag{13}$$

Journal of Newviews in Engineering and Technology (JNET)
Volume 5, Issue 4, December 2023
Available online at http://www.rsujnet.org/index.php/publications/2023-edition
e- ISSN: 2795-2215

Exergy inlet to compressor

$$E_{X,IN} = m_a[(h_2 - h_1) - T_1(s_2 - s_1)] = W_{C,Actual} \quad (14)$$

Exergy of products from compressor

$$I^R_{X.COMP} = m_a T_0\left[C_{pa}\ln\left(\frac{T_2}{T_1}\right) - R\ln\left(\frac{P_2}{P_1}\right)\right] \quad (15)$$

$$\eta_{\varepsilon,COMP} = \frac{E_{X,OUTPUT}}{E_{X,INPUT}} \, x\ 100 \quad (16)$$

Exergy inlet to combustion chamber

$$E_{X,IN} = m_a[(h_2 - h_0) - T_0(s_2 - s_0)] \quad (17)$$

Exergy of products from combustion chamber

$$E_{X,LOSS} = M_T T_0\left[C_{pt}\ln\left(\frac{T_3}{T_2}\right) - R\ln\left(\frac{P_3}{P_2}\right)\right] \quad (18)$$

$$\eta_{\varepsilon,COMB} = \frac{E_{X,OUTPUT}}{E_{X,INPUT}} \, x\ 100 \quad (19)$$

Exergy inlet to turbine

$$E_{X,IN} = m_g[(h_3 - h_0) - T_0(s_3 - s_4)] \quad (20)$$

Exergy of products from turbine

$$I^R_{X,T} = M_T T_0\left[C_{pt}\ln\left(\frac{T_4}{T_3}\right) - R\ln\left(\frac{P_4}{P_3}\right)\right] \quad (21)$$

$$E_{X,LOSS} = I^R_{M.T} + I^R_{X,T} \quad (22)$$

Exergy of products from exhaust

$$E_{X,LOSS} = M_T C_{pt}\left[(T_4 - T_0) - T_0 I_n\left(\frac{T_4}{T_0}\right)\right] \quad (23)$$

$$\eta_{\varepsilon,T} = \frac{E_{X,DESIRED}}{E_{X,INPUT}} \, x\ 100 \quad (24)$$

$$\eta_{th} = \frac{m_T C_{pt}(T_3 - T_4) - m_a C_{pa}(T_2 - T_1)}{m_T C_{pt}(T_3 - T_2)} \quad (25)$$

2.5 GPA Model

According to Yulong *et al*. (2015), the model-based GPA method has been widely used to monitor gas turbine engine health status because it can easily obtain the magnitudes of detected component faults with a thermodynamic performance model that relates gas path measurable (dependent) parameters such as temperatures, pressures, and shaft rotational speeds, among others, to fundamental component performance (independent) parameters. It is possible to express the thermodynamic relationship between engine gas path measurement parameters and engine component performance parameters as follows:

$$y = f(x) \quad (26)$$

But for multiple variables,

$$y_1 = f_1(x_1, x_2, x_3, \ldots x_n) \quad (26a)$$

Similarly,

$$y_2 = f_2(x_1, x_2, x_3, \ldots x_n) \quad (26b)$$

$$y_3 = f_3(x_1, x_2, x_3, \ldots x_n) \quad (26c)$$

$$y_n = f_n(x_1, x_2, x_3, \ldots x_n) \quad (26d)$$

Using ordinary differential equation, equations (26a,26b,26c and 26d) becomes.

$$\partial y_1 = \partial x_1 \frac{\partial f_1}{\partial x_1} + \partial x_2 \frac{\partial f_1}{\partial x_2} + \partial x_3 \frac{\partial f_1}{\partial x_3} + \ldots + \partial x_n \frac{\partial f_1}{\partial x_n} \quad (26e)$$

Similarly,

$$\partial y_2 = \partial x_1 \frac{\partial f_2}{\partial x_1} + \partial x_2 \frac{\partial f_2}{\partial x_2} + \partial x_3 \frac{\partial f_2}{\partial x_3} + \ldots + \partial x_n \frac{\partial f_2}{\partial x_n} \quad (26f)$$

$$\partial y_3 = \partial x_1 \frac{\partial f_3}{\partial x_1} + \partial x_2 \frac{\partial f_3}{\partial x_2} + \partial x_3 \frac{\partial f_3}{\partial x_3} + \ldots + \partial x_n \frac{\partial f_3}{\partial x_n} \quad (26g)$$

$$\partial y_n = \partial x_1 \frac{\partial f_n}{\partial x_1} + \partial x_2 \frac{\partial f_n}{\partial x_2} + \partial x_3 \frac{\partial f_n}{\partial x_3} + \ldots + \partial x_n \frac{\partial f_n}{\partial x_n} \quad (26h)$$

Equations (26e, 26f, 26g and 26h) can be solved and arranged to form the matrix shown below:

Journal of Newviews in Engineering and Technology (JNET)
Volume 5, Issue 4, December 2023
Available online at http://www.rsujnet.org/index.php/publications/2023-edition
e- ISSN: 2795-2215

$$J = \begin{bmatrix} \frac{\partial f_1}{\partial x_1} & \frac{\partial f_1}{\partial x_2} & \frac{\partial f_1}{\partial x_3} & \cdot & \cdot & \cdot & \frac{\partial f_1}{\partial x_n} \\ \frac{\partial f_2}{\partial x_1} & \frac{\partial f_2}{\partial x_2} & \frac{\partial f_2}{\partial x_3} & \cdot & \cdot & \cdot & \frac{\partial f_2}{\partial x_n} \\ \frac{\partial f_3}{\partial x_1} & \frac{\partial f_3}{\partial x_2} & \frac{\partial f_3}{\partial x_3} & \cdot & \cdot & \cdot & \frac{\partial f_3}{\partial x_n} \\ \cdot & \cdot & \cdot & \cdot & \cdot & \cdot & \cdot \\ \cdot & \cdot & \cdot & \cdot & \cdot & \cdot & \cdot \\ \cdot & \cdot & \cdot & \cdot & \cdot & \cdot & \cdot \\ \frac{\partial f_n}{\partial x_1} & \frac{\partial f_n}{\partial x_2} & \frac{\partial f_n}{\partial x_3} & \cdot & \cdot & \cdot & \frac{\partial f_n}{\partial x_n} \end{bmatrix}$$

This implies that.

$J\partial x = \partial y$

Let $\partial y = -F$

That is.

$$J\partial x = -F \tag{27}$$

$\partial x = (J^{-1}) - F$

Where,

J = Jacobian notation and stands for the first derivative in the Taylor series expansion

∂x = Dependent parameters change

∂y = Independent parameters change

J^{-1} = The fault coefficient matrix

Net power developed:

$$F_1 = m_a C_{pa} T_1 - m_a C_{pa} T_2 + (m_a C_{pa} + m_f C_{pf}) T_3 - (m_a C_{pa} + m_f C_{pf}) T_4 - P_T \tag{28}$$

Thermal efficiency for base load condition:

$$\eta_{th} = \frac{P_T}{M_T C_{pt}(T_3 - T_4)}$$

$$F_2 = T_3 - T_2 - \frac{P_T}{\eta_{th}(m_a C_{pa} + m_f C_{pf})} \tag{29}$$

Compressor isentropic efficiency

$$\eta_C = \frac{\text{Ideal isentropic work}}{\text{Actual work}} = \frac{T_{2s} - T_1}{T_2 - T_1}$$

$$F_3 = T_1 x_1 - T_1 + \eta_C T_1 - \eta_C T_2 \tag{30}$$

Turbine isentropic efficiency = η_T

$$\eta_T = \frac{\text{Actual work}}{\text{Ideal Isentropic work}} = \frac{T_3 - T_4}{T_3 - T_{4s}}$$

$$F_4 = T_3 - \frac{T_4}{\eta_T} - \frac{T_3}{x_1} - \frac{T_3}{\eta_T} \tag{31}$$

Differentiating Equations (28), (29), (30) and (31) with respect to x_1, T_2, T_3 and T_4, and substituting these values into (27) we can solve and arrange to form the matrix given below:

$$\begin{bmatrix} 0 & -m_a C_{pa} & (m_a C_{pa} + m_f C_{pf}) & -(m_a C_{pa} + m_f C_{pf}) \\ 0 & -1 & 1 & 0 \\ T_1 & -\eta_C & 0 & 0 \\ \frac{T_3}{x_1^2} & 0 & \left(1 - \frac{1}{x_1 -} - \frac{1}{\eta_T}\right) & \frac{1}{\eta_T} \end{bmatrix} \begin{bmatrix} \partial x_1 \\ \partial T_2 \\ \partial T_3 \\ \partial T_4 \end{bmatrix} = \begin{bmatrix} -F_1 \\ -F_2 \\ -F_3 \\ -F_4 \end{bmatrix} \tag{32}$$

3.0 RESULTS AND DISCUSSION

Table 1 shows the overall average exergy efficiency of the compressor as 78.534%. While exergy input due to compressor work was 217.485 MW and exergy out of the compressor at state-2 was 170.7991 MW, the average amount of exergy destroyed in the compressor is 46.686 MW. High exergy loss in the compressor is caused by clogged inlet air filters that cause high differential air pressures and increase in surface roughness. This is due to dirt deposits on compressor blades which changes the air flow patterns and causes the compressor to use more gas turbine power to compress the same amount of air. The original equipment manufacturer (OEM) recommends an off-line compressor wash when power output is reduced by 5% - 8% of normal power output and an on-line compressor wash after off-line cleaning on a regular basis to keep power output loss to less than 2% - 4%. It was discovered that neither of these were strictly followed, which was a major contributor to the high deposit of dirt on compressor blades.

From Table 2, the combustion chamber exergy destroyed rate was greater than that of the other plant components, at 108.3278 MW with an exergy efficiency of 78.724%. The total amount of exergy inflow into the combustion chamber was found to be 509.158 MW, with 338.3589 MW coming from exergy in the fuel and 170.7991 MW coming from the compressor alone. This is validated by Lebele-Alawa and Asuo (2013). According to their findings, the

Journal of Newviews in Engineering and Technology (JNET)
Volume 5, Issue 4, December 2023
Available online at http://www.rsujnet.org/index.php/publications/2023-edition
e- ISSN: 2795-2215

combustion chamber has the highest rate of exergy destruction, followed by the exhaust section, compressor, and turbine. The high rate of exergy loss is caused by high irreversibilities in the combustion chamber.

Table 1: Summary of results for Exergy Analysis of Compressor

S/N	Description	Value (MW)
1	Exergy Inflow, $E_{X,\,IN}$	0
2	Exergy due to Compressor Work, $W_{C,\,ACTUAL}$	217.485
3	Exergy Outflow, $E_{X,\,OUT}$	170.7991
4	Exergy Destroyed, $E_{X,\,Des}$	46.686
5	Exergetic Efficiency of Compressor, [illegible]	78.534 %

Table 2: Summary of results for Exergy Analysis of Combustion Chamber

S/N	Description	Value (MW)
1	Exergy Inflow, $E_{X,\,IN}$	170.7991
2	Exergy of Fuel, $E_{X,\,FUEL}$	338.3589
3	Exergy Outflow, $E_{X,\,OUT}$	400.8302
4	Exergy Destroyed, $E_{X,\,Des}$	108.3278
5	Exergetic Efficiency of Combustion, [illegible]	78.724 %

In Table 3, the turbine section exergy destruction rate was the lowest compared to other plant components, with a value of 44.1815 MW and the highest exergy efficiency of 88.9775%. The exergy inflow into the turbine was 400.8302 MW, with an exergy outflow of 79.4598 MW. The turbine's performance was measured by the ratio of turbine exergy outflow to turbine exergy inflow to the turbine section. Mechanical frictional losses, turbine inter-stage leakages, and worn seals all contributed to the exergy loss.

Table 3: Summary of results for Exergy Analysis of Turbine

S/N	Description	Value (MW)
1	Exergy Inflow, $E_{X,\,IN}$	400.8302
2	Exergy Outflow, $E_{X,\,OUT}$	79.4598
3	Exergy Destroyed, $E_{X,Des}$	44.1815
4	Exergetic Efficiency of Turbine, [illegible]	88.9775 %

The results of Table 4 revealed that the amount of exergy inflow to the exhaust equals the amount of exergy destroyed, which was 79.4598 MW for the exhaust section. Because the flue gas is channeled directly to the exhaust stack via the diffuser, this high exergy loss is primarily due to unutilized high flue gas temperatures.

Table 4: Summary of results for Exergy Analysis of Turbine Exhaust

S/N	Description	Value (MW)
1	Exergy Inflow, $E_{X,\,IN}$	79.4598
2	Exergy Outflow, $E_{X,\,OUT}$	0.0000
3	Exergy Destroyed, $E_{X,\,Des}$	79.4598

3.1 Overall Plant Exergy Analysis

For each component of the plant, the sum of exergy inflows and exergy lost equals zero. These zero sums demonstrate that the component exergy balances were completed correctly to satisfy the flow conditions. The power plant's analysis revealed that the highest

Journal of Newviews in Engineering and Technology (JNET)
Volume 5, Issue 4, December 2023
Available online at http://www.rsujnet.org/index.php/publications/2023-edition
e- ISSN: 2795-2215

Exergy losses occur in the combustion chamber and exhaust, followed by the compressor, and the lowest in the turbine section. However, it is worth noting that the value of 217.4851 MW listed as exergy in-flow to the compressor in Table 5 represents the actual work done on the compressor by the turbine because there is no exergy flow to the compressor. In addition, the average plant exergy efficiency is 54.729%.

3.2 Compressor Non-linear Gas Path Analysis (GPA)

Table 6 shows that the variation of the average actual compression ratio was 11.091 and the variation of the average calculated compression ratio was 14.34, giving a deviation of 22.66%. The average actual and calculated compressor exit temperatures are 381.821^{0}C and 431.48024 ^{0}C, with 11.51% deviation. High deviations indicate more severe deterioration. With low ambient inlet temperatures, total power output increases as compression ratio increases. When compared to the calculated (modelled) state, the low compression ratio and compressor exit temperatures indicate an unhealthy state of the compressor.

Table 5: Summary of Net Flow of Exergy Across Boundaries of Machine Components

S/N	Process	Ex_{IN} (MW)	Ex_{OUT} (MW)	Ex_{LOSS} (MW)	$W_T$actual (MW)	Ex. Eff. (%)
1.	Compression (1-2)	217.4851	170.7991	46.686	-	78.534
2.	Combustion (2-3)	509.158	400.8302	108.3278	-	78.724
3.	Turbine (3-4)	400.8302	79.4598	44.1815	277.1889	88.9775
4.	Exhaust (4-1)	79.4598	0.0000	79.4598	-	0.0000
5.	Overall Average Exergetic Efficiency					81.922
6.	Overall Average Net Efficiency					36.997

Table 6: Summary of average actual and calculated dependent parameters and their deviations.

S/N	Parameter	Actual Value (Log Sheet)	Calculated Value	Unit	Deviation (%)
1.	Compression Ratio (P_2/P_1)	11.0910	14.3400	-	22.66
2.	Compressor Exit Temp (T_2)	381.8210	431.48024	^{0}C	11.51
3.	Turbine Inlet Temp (T_3)	1002.9950	1005.94124	^{0}C	0.30
4.	Turbine Outlet Temp (T_4)	431.6653	393.5966	^{0}C	9.672

3.3 Combustion Chamber Non-linear Gas Path Analysis

Table 6 also compares the actual compression ratio (11.091) and compressor exit temperature (381.821^{0}C) to the calculated (ideal) compression ratio (14.34) and compressor exit temperature (431.48024^{0}C), resulting in actual and calculated turbine average inlet temperatures of 1002.995 ^{0}C and 1005.94124 ^{0}C, respectively, with a 0.3% deviation (variation in combustion chamber temperature). Because the rate of fuel gas supply is directly proportional to the load, the high irreversibility in the combustion chamber is caused by fluctuating load (part load) demands, which affects fuel gas supply pressures (output power). That is, because the pressure of the fuel gas supply is not constant, any variations in system fuel supply will result in venting the excess gas, wasting exergy.

3.4 Turbine Section Non-linear Gas Path Analysis

Table 6 shows that the average actual turbine inlet or firing temperature is 1002.995^{0}C, while the average calculated, or ideal firing temperature is 1005.94124^{0}C. It is well known that the higher the firing temperature of a gas turbine, the higher the unit efficiency. As a result, a 0.30% change from the machine's healthy to unhealthy state will result in a decrease in unit efficiency.

Journal of Newviews in Engineering and Technology (JNET)
Volume 5, Issue 4, December 2023
Available online at http://www.rsujnet.org/index.php/publications/2023-edition
e- ISSN: 2795-2215

The average actual and calculated turbine exit temperatures were 431.6653 ^{0}C and 393.5966 ^{0}C, respectively, indicating that the actual exit temperature is higher than expected with a hot gas temperature deviation of 9.672%, indicating that machine performance is limited by this variation, which could be due to turbine inter-stage leakages or worn rotor and stator heat shields and seals allowing unutilized hot gases to escape directly into the exhaust diffuser.

Table 7: Summary of Average Turbine Inlet and Outlet Temperatures and their deviations.

	Parameter	Actual Value	Calculated Value	Deviation (%)
1	Average Turbine Inlet Temp, T_3	1002.995 ^{0}C	1005.94124 ^{0}C	0.30
2	Average Turbine Outlet Temp, T_4	431.6653 ^{0}C	393.5966 ^{0}C	9.672

Table 8: Summary of Components Average Exergy Destruction Rates.

S/N	Component	Exergy Destroyed (MW)	Value(%)
1	Compressor	46.6860	16.75
2	Combustion Chamber	108.3278	38.88
3	Turbine	44.1815	15.86
4	Exhaust	79.4598	28.52

3.5 Exhaust Non-linear Gas Path Analysis

According to the results in Table 7 the actual turbine exit temperature was 431.6653 ^{0}C and the calculated turbine exit temperature was 393.5966 ^{0}C. With a deterioration rate of 9.672%, this indicates heat energy loss due to high temperature differences because the actual exhaust temperature is higher than the calculated exhaust temperature (healthy condition). This could be due to the turbine not utilizing available energy to do work because of increased blade clearance and worn seals. Exhaust temperatures that are higher than normal will reduce power output and efficiency. This is supported by the findings of Parapa (2021), establishing those changes in exhaust temperature parameter of 1^{0}C has an impact on decreasing the power output by 0.273% and increasing the heat rate by 0.047%.

4.0 CONCLUSION

This study's analysis of the performance of the 180 MW Afam Rivers IPP power plant using exergy and non-linear gas path analysis models reveals that the combustion chamber's exergy destruction rate (108.3278 MW) is significantly higher than that of the other parts of the system because of the combustion chamber's high fuel exergy and the chemical reactions between the air and fuel mixtures. The analysis also identifies where and how much energy is lost during each of the Brayton cycle's thermodynamic processes. Combustion chamber, exhaust section, compressor, and turbine losses are the largest and are attributed to irreversibilities, improper maintenance, mechanical loss, metallurgical component limitations at high temperatures, and hot gas leaks.

The turbine has the highest energy efficiency (88.9775%) and the lowest loss rate. With over 40,000 operating hours (OH) and an equivalent operating hour (EOH) of approximately 116,000, the Afam GT13E2 (1 x 180 MW) power plant has been in operation for almost ten years. Only one major inspection (major overhaul), which is supposed to be performed every 36,000 EOH, has been completed (OEM recommendation). When compared to base load operating conditions, the machine's efficiency has decreased by 3.93% because of the failure to perform proper maintenance when it was required. In terms of temperature difference (11.51%), compression ratio (22.66%), and temperature difference (9.672%)

Journal of Newviews in Engineering and Technology (JNET)
Volume 5, Issue 4, December 2023
Available online at http://www.rsujnet.org/index.php/publications/2023-edition
e- ISSN: 2795-2215

in the turbine section, the degradation was more pronounced in the compressor section. This degradation is because of compressor fouling from clogged inlet air filters, blade tip clearances, dysfunctional burners, and gas control valves. Low power output, firing temperature, and compression ratio were all results of compressor fouling. The two methods used in this analysis were compared, and it was found that the exergy analysis method, which uses the first and second laws of thermodynamics to measure energy quantity and quality, is preferred to the non-linear gas path analysis method, which only measures energy quantity and is restricted to the first law of thermodynamics.

5.0 ACKNOWLEDGEMENTS

The authors would want to express their gratitude to Professor J. I. Sodiki, Dr. R. K. C. Amadi, Dr. F. E. Oparadike and Dr. J. M. Asuo, for their support.

NOMENCLATURE

c_1 Velocity of fluid at inlet (m/sec)

c_2 Velocity of fluid at outlet (m/sec)

C_{pa} Specific heat capacity of air at constant pressure (kJ/kg. K)

C_{pf} Specific heat capacity of fuel (kJ/kg. K)

C_{pt} Specific heat capacity of air-fuel mixture (kJ/kg. K)

$E_{X,Desired}$ Sum of useful exergy outputs (MW)

$E_{X,T}$ Total exergy (kJ)

$E_{X,PH}$ Physical exergy (kJ)

$E_{X,CH}$ Chemical exergy (kJ)

$E_{X,KN}$ Kinetic exergy (kJ)

$\sum W$ Sum of ideal work (kJ)

$\sum Q$ Sum of heat supplied (kJ)

$\sum E_{X,IN}$ Sum of exergy inflow (kJ)

$\sum E_{X,OUT}$ Sum of exergy outflow (kJ)

$\sum E_{X,Dest.}$ Sum of exergy loss in the system due to irreversibilities. (kJ)

$\sum E_{X,FUEL}$ Exergy sums of fuel (kJ)

$\sum E_{X,LOSS}$ Rate of exergy loss (kJ)

h_0 Specific enthalpy of stream at reference state (kJ/kg)

h_1 Specific enthalpy of stream entering the compressor (kJ/kg)

h_2 Specific enthalpy of stream leaving the compressor (kJ/kg)

h_3 Specific enthalpy of stream entering the turbine (kJ/kg)

h_4 Specific enthalpy of stream leaving the turbine (kJ/kg)

$I^R_{X,COMP}$ Exergy loss due to irreversibilities in the compressor (MW)

$I^R_{M,COMP}$ Mechanical irreversibilities in the compressor (MW)

$I^R_{M,T}$ Mechanical irreversibilities in the Turbine (MW)

$I^R_{X,T}$ Exergy loss due to irreversibility in the Turbine (MW)

J^{-1} The fault coefficient matrix

m_a Mass flow rate of air stream entering the compressor (kg/sec)

m_f Mass flow rate of fuel (kg/sec)

M_T Mass flow rate of air-fuel mixture (kg/sec)

p_0 Reference Pressure (bar)

p_1 Compressor Inlet Pressure (bar)

p_2 Compressor Discharge Pressure (bar)

p_3 Gas Inlet Pressure to Turbine (bar)

p_4 Gas Outlet Pressure from Turbine (bar)

Q_{CMB} Heat supplied in the combustion chamber (MW)

R Gas constant (kJ/kg. K)

r_p Compression Ratio

Specific Entropy of Stream at Reference State (kJ/kg. K)

Journal of Newviews in Engineering and Technology (JNET)
Volume 5, Issue 4, December 2023
Available online at http://www.rsujnet.org/index.php/publications/2023-edition
e- ISSN: 2795-2215

s_1 Specific Entropy of Stream Entering the Compressor (kJ/kg. K)
s_2 Specific Entropy of Stream Leaving the Compressor (kJ/kg. K)
s_3 Specific Entropy of Stream Entering the Turbine (kJ/kg. K)
s_4 Specific Entropy of Stream Leaving the Turbine (kJ/kg. K)
T_0 Reference Temperature (K)
T_1 Compressor Inlet Temperature (K)
T_2 Compressor Discharge Temperature (K)
T_{2s} Ideal Compressor Discharge Temperature (K)
T_3 Gas Inlet Temperature to Turbine (K)
T_4 Gas Outlet Temperature from Turbine (K)
T_{4s} Ideal Turbine Outlet Temperature (K)
u_1 Specific Internal Energy at Inlet (kJ/kg)
u_2 Specific Internal Energy at Outlet (kJ/kg)
v_1 Specific Volume at Inlet (m^3/kg)
v_2 Specific Volume at Outlet (m^3/kg)
W_2 Compressor Work Input (kJ/kg)
$W_{C,IDEAL}$ Ideal Compressor Work (kJ/kg)
$W_{C,ACTUAL}$ Actual Compressor Work (kJ/kg)
W_T Turbine Work Output (kJ/kg)
$W_{T,IDEAL}$ Ideal Turbine Work (kJ/kg)
$W_{T,ACTUAL}$ Actual Turbine Work (kJ/kg)
Z_1 Elevation at Inlet (m)
Z_2 Elevation at Outlet (m)

Greek Symbols
∂x Dependent parameters change
∂y Independent parameters change
η_C Compressor isentropic efficiency
η_T Turbine isentropic efficiency η_X Exergetic efficiency
η_{th} Net thermal efficiency
γ Polytropic index of air

Subscripts
0 Reference state
1 Compressor inlet state
2 Compressor outlet and combustion chamber inlet state
3 Combustion chamber outlet and turbine inlet state

REFERENCES

Baheta, A. T. & Gilani, S. I. (2011). Exergy based performance Analysis of a Gas Turbine at part load conditions. *Journal of Applied sciences*, 11(11), 1994 – 1999.

Horlock, J. H., (2003). *Advanced Gas Turbine Cycles*. Whittle laboratory, Cambridge, U.K. Elsevier Science ltd. ISBN:0-08-044273-0

Lebele-Alawa, B. T. & Jerry M. A. (2011). Exergy Analysis of Kolo-Creek Gas Turbine Plant. 14. *Canadian Journal on Mechanical Sciences and Engineering. 2(8), 14 – 24.*

Lebele-Alawa, B. T., & Asuo, J. M., (2013). Performance Analysis of 20 MW Gas Turbine Power Plant by Energy and Exergy methods. *Journal of Applied Science and Technology (JAST)*, 18 (1&2), 20-26.

Okechukwu, E. H, & Imuentinyan, O. A., (2013). Exergy Analysis of Omotosho Phase-1 Gas Thermal Power Plant. *International Journal of Energy and Power Engineering*, 2, (5) 197-203.

Oyedepo, S. O., Adefila, R. O. & Fagbenle, M. (2015). Performance Evaluation of selected gas Turbine power plants in Nigeria using Energy and Exergy Methods. *World Journal of Engineering*, 3(3), 239 – 256.

Parapa, H. B. P. (2021). The impact of changes in exhaust temperature on the power output and heat rate of a gas turbine with a capacity of 238 MW. *INTEK Journal Penelitian,* 8(2), 96-100.

Stamatis, A. G. (2010). Evaluation of gas path analysis methods for gas turbine diagnosis, department of mechanical engineering, university of Thessaly, Greece. *Journal of mechanical science and technology*, 25(2), 1207-1209.

Verbist, M. L. (2017). Gas path analysis for enhanced aero-engine condition monitoring and maintenance. (PhD Thesis). Delft University of Technology, Netherlands.

Yulong, Y., Yunpeng, C., Shuying, L., & Jingchao, L. (2015). Non-linear steady state model-based gas turbine health status estimation approach with improved particle swarm optimization algorithm. College of power and energy engineering, Harbin engineering university, Harbin, China. http://dx.doi.org/10.1155/2015/940757

Journal of Newviews in Engineering and Technology (JNET)
Volume 5, Issue 4, December 2023
Available online at http://www.rsujnet.org/index.php/publications/2023-edition
e- ISSN: 2795-2215

Plant Technical Data Sheet-1

ABCD

GT13E2 Gas Turbine - Thermal Block
Open Cycle Power Plant - Port Harcourt 1

4 Technical Data

Criteria	
Plant name:	Open Cycle Power Plant - Port Harcourt 1
Machine No:	G322
Type:	GT13E2
Year of manufacture:	2010
Fuel type:	Natural gas, dry operation
Nominal speed:	3000 rpm
GT power output (at design ambient conditions):	160.0 MW
Direction of rotation:	Clockwise (viewed on intake end)
Design ambient pressure:	1.013 bar
Design ambient air temperature:	31 °C
GT exhaust mass flow	528 kg/s
(at design ambient conditions): Compressor stages:	21
Turbine stages:	5
No. of combustion chambers:	1
Combustion chamber type:	Single annular
No. of burners:	72
GT turbine inlet temperature (TIT), max:	1095 °C (base load)
Overall length:	10.78 m
Rotor diameter, max:	4.5 m
Mass:	320 t
Rotor barring speed:	<1 rpm

Table 2 Technical data

Journal of Newviews in Engineering and Technology (JNET)
Volume 5, Issue 4, December 2023
Available online at http://www.rsujnet.org/index.php/publications/2023-edition
e- ISSN: 2795-2215

Plant Technical Data Sheet-2

Port Harcourt

Calculated GT Performance on Natural Gas

Parameter	Unit	Case 1	Case 2	Case 3
		Min.	Baseload	Max.
Conditions				
Ambient air temperature	°C	13.00	31.00	41.00
Ambient air humidity	%	83.00	70.00	70.00
Ambient pressure	bar	1.013	1.013	1.013
Inlet pressure drop (Ref. value)	mbar	Included	Included	Included
Outlet pressure drop (Ref. value)	mbar	1.96	1.76	1.59
GT load	%	100	100	100
Grid frequency	Hz	50	50	50
Generator power factor (cos phi)	1	0.85	0.85	0.85
GT Power, GT Exhaust				
GT net power output	MW	180.00	160.00	147.66
GT exhaust temperature	°C	499	514	527
GT exhaust massflow	kg/s	562	528	498
Fuel				
Fuel Source	-	Normal Gas	Normal Gas	Normal Gas
Lower heating value of fuel	kJ/kg	48461.7	48461.7	48461.7
Fuel temperature	°C	33.00	33.00	33.00
Sensible heat of fuel (t_ref = 15°C)	kJ/kg	37.64	37.64	37.64
Fuel mass flow	kg/s	9.8	9.1	8.7
Exhaust Gas Composition				
Mole-fraction of N2 in exhaust	kmol/kmol	0.749077	0.735130	0.717948
Mole-fraction of O2 in exhaust	kmol/kmol	0.141292	0.138328	0.133835
Mole-fraction of H2O in exhaust	kmol/kmol	0.069192	0.086683	0.108630
Mole-fraction of CO2 in exhaust	kmol/kmol	0.031478	0.031067	0.030999
Mole-fraction of Ar in exhaust	kmol/kmol	0.008960	0.008793	0.008587
Mole-fraction of SO2 in exhaust	kmol/kmol	0.000000	0.000000	0.000000